This is the accepted manuscript made available via CHORUS. The article has been published as:

Phase evolution in the ferroelectric relaxor Ba(Ti_{1−x},Zr_{x})O_{3} from atomistic simulations

C. Mentzer, S. Lisenkov, Z. G. Fthenakis, and I. Ponomareva

Phys. Rev. B **99**, 064111 — Published 25 February 2019

DOI: 10.1103/PhysRevB.99.064111

Phase evolution in $Ba(Ti_{1-x},Zr_x)O_3$ ferroelectric relaxor from atomistic simulations

C. Mentzer,[1] S. Lisenkov,[1] Z. G. Fthenakis,[1] and I. Ponomareva[1]

[1] *Department of Physics, University of South Florida, Tampa, Florida 33620, USA*

Abstract

We develop and/or use a combination of first-principles Density Functional Theory and first-principles-based effective Hamiltonian approaches to investigate phase evolution in $Ba(Ti_{1-x},Zr_x)O_3$ ferroelectric relaxor. Our simulations reveal two competing effects, which are associated with substitution of Ti with Zr and primarily responsible for the unusual phase evolution and properties of this family of solid solutions. They are the negative chemical pressure that Zr exerts on the $BaTiO_3$ matrix and the ferroelectric "inactivity" of Zr itself. While the former one has stabilizing effect on ferroelectricity, the latter one disrupts the ferroelectric cooperation. These competing effects are responsible for the so-called pinched phase transition, where the three phases of parent $BaTiO_3$ merge together, and the loss of ferroelectricity at the onset of relaxor behavior. The origin of the controversial diffuse phase transition is attributed to the coexistence of the three ferroelectric phases. In the region of the diffuse phase transition we detect polar nanoregions, which often exhibit unusual nanopillar geometry.

INTRODUCTION

Ferroelectric solid solutions such as $Pb(Ti_{1-x},Zr_x)O_3$, $Ba(Ti_{1-x},Zr_x)O_3$, $(Ba_{1-x},Sr_x)TiO_3$ exhibit excellent ferroelectric, pyroelectric, and piezoelectric properties and find numerous applications in capacitors, nonlinear optical devices, piezoelectric transducers, ultrasonic imaging, common rail fuel injection systems, energy harvesting devices, just to name a few [1, 2]. Their unique feature is high tunability of these properties by varying concentration. Among different solid solutions the family of $Ba(Ti_{1-x},Zr_x)O_3$ solid solutions stands out because of their lead-free nature and extreme richness of phase diagram. The parent compound $BaTiO_3$ exhibits a sequence of phase transitions: paraelectric cubic to ferroelectric tetragonal at 393 K, ferroelectric tetragonal to ferroelectric orthorhombic at 278 K, and ferroelectric orthorhombic to ferroelectric rhombohedral at 183 K [3]. As the Zr concentration in these compounds increases the multiple phase transitions of parent $BaTiO_3$ merge giving rise to the so-called pinched transition around x =0.10 [3] (see Fig.4(b)). Interestingly, while the existence of pinched transition region is well established experimentally, there is a lack of microscopic understanding of the driving force behind the phase transitions merging. How does paraelectric $BaZrO_3$ stabilize the ferroelectric rhombohedral phase? In contrast, in other $BaTiO_3$-based solid solutions, $(Ba_{1-x},Sr_x)TiO_3$, the transition temperatures for all three ferroelectric phase transitions decreases gradually with the increase of $SrTiO_3$ content [4, 5].

In the concentration range of 0.10 to 0.20 the $Ba(Ti_{1-x},Zr_x)O_3$ undergoes a single phase transition from the paraelectric cubic to ferroelectric rhombohedral phase. However, the associated peak in the dielectric susceptibility is much broader than in $BaTiO_3$ which sometimes is referred to as diffuse phase transition [3]. The nature of the diffuse phase transition is rather controversial as some believe that such transition is the signature of the relaxor state [6], while other experimental evidence suggests that the diffuse phase transition is actually associated with a ferroelectric phase transition owing to the observation of the ferroelectric domains in the vicinity of the temperature T_m associated with maximum in dielectric constant [7]. At higher substitutions of >0.20 of Zr T_m shows frequency dependence, which is a hallmark of relaxor behavior. Such signature property of relaxors is attributed to the existence of polar nanoregions (PNRs) which are nanoscopic regions of locally correlated polarization that appear at the "Burns" temperature. The microscopic origins of

PNRs are typically related to the structural and charge inhomogeneities present in relaxors. However, the onset of relaxor behavior in systems without nominal charge disorder, like in $Ba(Ti_{1-x},Zr_x)O_3$ case is not well understood [3]. It is believed that broad distribution of PNR sizes and their dynamical nature give rise to broad distribution of relaxation times and consequently broad dielectric response. In $Ba(Ti_{1-x},Zr_x)O_3$ in the compositional range 0.25 to 0.35 of Zr a percolation transition occurs below a temperature associated with the freezing of polar nanoregions. In the range of x from 0.35 to 0.80 canonical nonergodic relaxor behavior occurs with macroscopic cubic symmetry.

Clearly addressing these questions and controversies at the fundamental level requires atomistic insights from first-principles-based finite-temperature dynamical simulations. In a recent study [8] a first-principles-based approach was developed to investigate $Ba(Ti_{1-x},Zr_x)O_3$ solid solutions with x =0.5. The static simulations indicated that the random fields and random strains do not play a major role in the relaxor behavior of this solid solution. The study attributed the relaxor state to the difference in the ferroelectric strength between Ti and Zr ions as well as the importance of antiferroelectriclike interactions. A follow up study revealed a field-induced percolation of polar nanoregions in this material [9]. In contrast, another recent atomistic study looked at the dynamics of relaxor $75\%PbMg_{1/3}Nb_{2/3}O_3$-$25\%PbTiO_3$ and proposed a model of anisotropic local correlations that contradicts the polar nanoregion model [10]. The study of high-frequency dynamics in $Ba(Ti_{1-x},Zr_x)O_3$ led to the prediction of an exotic fanoresonance [11]. More recently some $Ba(Ti_{1-x},Zr_x)O_3$ solid solutions were studied at zero Kelvin with first-principles simulations [12]. It was found that Zr substitution of Ti strongly favors short-range repulsive force. On the other hand, the bigger size of Zr locally favors the long-range interactions along O-Ti-O-Ti-O chains. At the same time, to the best of our knowledge, no microscopic insight is available for the region associated with the crossover between the ferroelectric, diffuse ferroelectric and relaxor state, which is, in our opinion, instrumental for understanding of the relaxor state in systems without nominal charge disorder.

The aims of this work are i) to develop first-principles-based computational approach capable of modeling this family of solid solutions in a wide compositional and temperature range; ii) to apply this computational approach along with first-principles zero Kelvin simulations to elucidate the phase evolution in these solid solutions; iii) to address some of the aforementioned questions and controversies.

METHODOLOGY

We begin by investigating two compositions of $Ba(Ti_{1-x},Zr_x)O_3$, x =0.0 and x =0.125, at zero Kelvin using first-principles Density Functional Theory (DFT) calculations. Vienna simulation package (VASP) [13] was used with projector augmented wave method [14]. The Kohn-Sham equations were solved using local density approximation. We used the cut-off energy of 500 eV which yielded good convergence. For electronic structure calculation Monkhorst-Pack 8x8x8 mesh was chosen. The simulation supercell contained 2x2x2 cubic perovskite unit cells of $BaTiO_3$. For $Ba(Ti_{0.875},Zr_{0.125})O_3$ one of the Ti in the supercell was replaced with Zr.

All structural optimizations of the supercells were carried out until the forces on the ions were less than 10^{-4} eV/Å and the stresses were less than 0.1 kbar. Both structures were investigated in their cubic $Pm\bar{3}m$ phase and $R3m$ ground state. The polarization was calculated using the Berry phase approach [15] and the ionic displacements. In the latter one the polarization was computed from $P = Z^*\Delta u/V$, where Z^* is the Born effective charge for the ions and u is half the ionic displacements associated with polarization reversal. We used the following values for the Born effective charges $Z^*_{Ba} = 2.75$, $Z^*_{Zr} = 6.11$, $Z^*_{Ti} = 7.40$, $Z^*_{O1} = -5.82$, $Z^*_{O2} = -2.16$ that were found from DFT calculations. In the ground state of $BaTiO_3$ the polarization is aligned along <111> crystallographic direction and has a value of 30.0 μC/cm^2 from Berry phase calculations and 31.8 μC/cm^2 from the ionic displacements computations. These values compare well with the experimental value of 33.5 μC/cm^2 [16].

To elucidate the atomistic effect of Ti substitution with Zr we replaced one of the Ti with Zr in both cubic and ground state phases of the $BaTiO_3$ and computed the associated forces that are shown schematically in Fig.1. This corresponds to $Ba(Ti_{0.875},Zr_{0.125})O_3$. In both the cubic and c phases Zr pushes surrounding atoms away due to its larger ionic size, which ultimately leads to the lattice expansion. In addition, in $R3m$ phase we find a relatively large force on Zr. The direction of the force indicates that this is a restoring force that acts to return Zr to its undistorted position revealing its inability to polarize with the rest of the lattice. Next both supercells were relaxed through optimization of ionic positions and supercell size. The resultant ionic displacements are consistent with the force patterns. In the cubic phase of $Ba(Ti_{0.875},Zr_{0.125})O_3$ we find 0.75% increase of the lattice constant with respect to $BaTiO_3$ which corresponds to -3.64 GPa pressure applied to $BaTiO_3$. Negative

pressure has stabilizing effect on ferroelectricity as it shifts the energy balance in favor of long range Coulomb interactions. In $R3m$ phase of $Ba(Ti_{0.875},Zr_{0.125})O_3$ the polarization is 26.0 $\mu C/cm^2$ from Berry phase calculations and 31.3 $\mu C/cm^2$ from the ionic displacements.

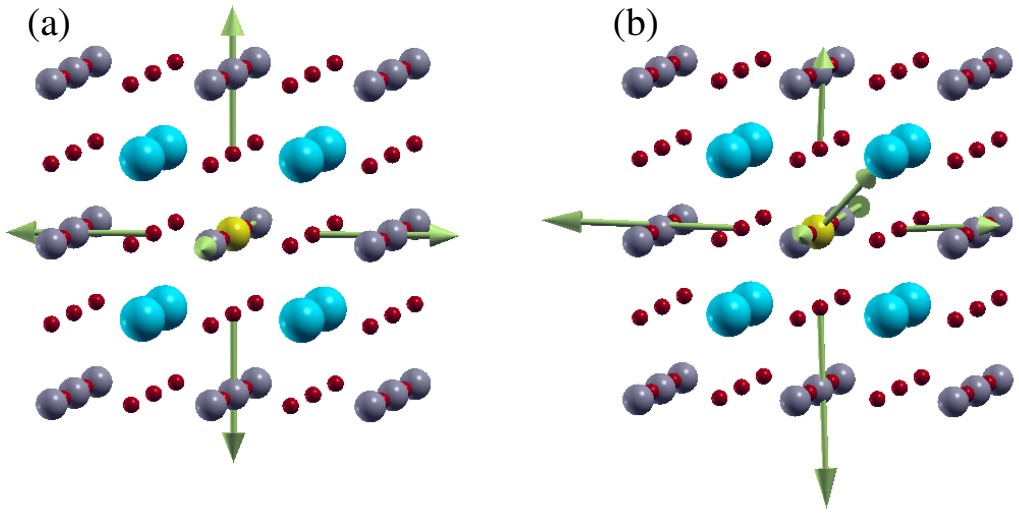

FIG. 1. Schematic representation of the forces acting on Zr substitution in $BaTiO_3$ cubic phase (a) and ground state (b).

We have used the ionic displacements approach to compute local polarization in the $R3m$ phase of $Ba(Ti_{0.875},Zr_{0.125})O_3$ and compare it to the one in $BaTiO_3$. The polarization vector was taken to be centered on the Ti- or Zr-site. The results are shown schematically in Fig.2. The most prominent feature is the extremely small polarization on the Zr site (only $0.3P_{BTO}$) which confirms that Zr does not like to polarize. For the Zr nearest neighbour unit cells along <100> the polarization direction deviates significantly from the <111> and is almost along <011>. Interestingly, for Ti unit cells we find enhancement of local polarization in comparison with $BaTiO_3$ (about 1.12 P_{BTO}).

Thus our simulations demonstrate that larger Zr pushes away its surrounding ions which leads to the lattice expansion (chemical pressure). Zr, however, does not participate in the collective distortions of the $BaTiO_3$ lattice that give origin to the polar phase. Quite surprisingly, Zr plays a dual role: it favors ferroelectricity through exerting negative chemical

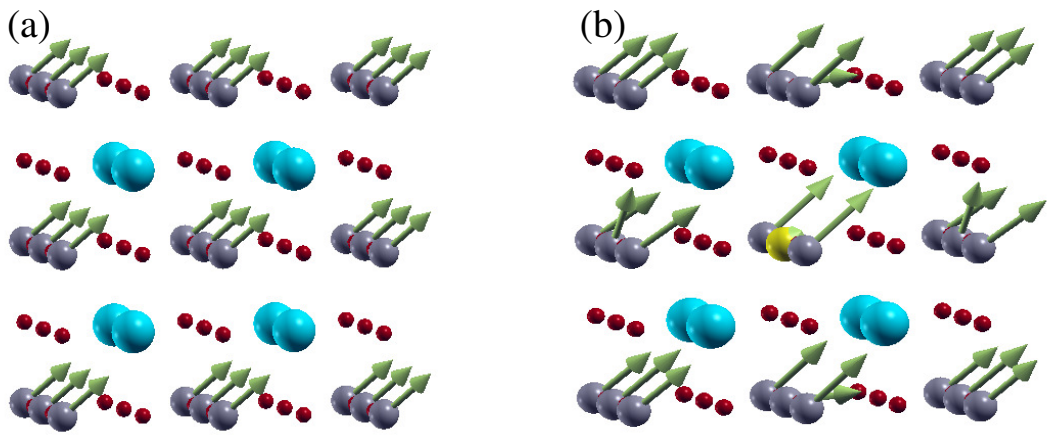

FIG. 2. Schematic representation of the local polarization in $BaTiO_3$ (a) and $Ba(Ti_{0.875},Zr_{0.125})O_3$ (b).

pressure on the $BaTiO_3$ matrix (mechanical effect), while simultaneously weakens the ferroelectric interactions by not participating in the collective distortion (electrostatic effect). These findings are in line with previous computational studies [8, 12].

In order to study the phase evolution in a wide concentration range and at finite temperatures we extend the first-principles-based effective Hamiltonian of Ref.17 to the case of $Ba(Ti_{1-x},Zr_x)O_3$ with low Zr concentration. The degrees of freedom for the Hamiltonian include local modes, $\mathbf{u}_i$, that are proportional to the dipole moment in the unit cell, and strain variables tensors η_i (in Voigt notations) that are responsible for mechanical deformations of a unit cell. The energy of the Hamiltonian is [17]

$$E^{\text{tot}} = E^{\text{FE}}(\{\mathbf{u}_i\}) + E^{\text{elas}}(\{\eta_i\}) + E^{\text{FE-elas}}(\{\mathbf{u}_i, \eta_i\}) + E^{elec}(\{\mathbf{u}_i\}), \quad (1)$$

where E^{FE} is the energy associated with the ferroelectric local modes and includes contributions from the dipole-dipole interactions, short-range interactions, and on-site self energy as defined in Ref.18. The second term, E^{elas}, is the elastic energy associated with the unit cell deformations. $E^{\text{FE-elas}}$ is the energy contribution due to the interactions between the ferroelectric local modes and the strain. The last term, $E^{elec}(\{\mathbf{u}_i\}) = Z^* \sum_i \mathbf{E} \cdot \mathbf{u}_i$, gives the interaction energy between the local modes and an external electric field, $\mathbf{E}$.

To extend the Hamiltonian to the case of $Ba(Ti_{1-x},Zr_x)O_3$, we recall that DFT calculations revealed that Zr does not participate in the collective displacement that gives origin to the spontaneous polarization in $BaTiO_3$. This means that if displaced, it experiences a restoring force. We computed the restoring force acting on the local mode centered on Zr as follows $\mathbf{F_u} = \sum_i (\mathbf{F}_i^{rho} - \mathbf{F}_i^{cubic})\xi_i$. Here $\mathbf{F}_i^{rho}$ and $\mathbf{F}_i^{cubic}$ are the forces on the ion i surrounding Zr in the $R3m$ and cubic phase, respectively. Zr itself is also included in the summation. These forces are obtained from DFT calculations. ξ_i are the components of the eigenvector associated with the unstable polar mode of $BaTiO_3$. They are ξ_{Ba} =-0.25, ξ_{Ti} =-0.74, $\xi_{O_1} = 0.52$, $\xi_{O_2} = 0.24$ [19]. Note, that we subtract forces acting on the ions in the cubic phase in order to separate the electrostatic and mechanical effects of Ti substitution. This force was then used to calculate the restoring force constant $k_{Zr} = -F_z/2u_z$, where u_z is the Cartesian component of the local mode. The associated harmonic term in the effective Hamiltonian is $\sum_j k_{Zr}(u_x^2(j) + u_y^2(j) + u_z^2(j))$, where k =0.17213 Ha/Bohr^2 and j runs over all unit cells that contain Zr.

To model the lattice expansion of due to presence of Zr we simulate hydrostatic pressure that depends on Zr concentration as follows $P = -22 \times x$ GPa, which was found on the basis of first-principles calculations. More specifically, we ran DFT simulations with 1 through 8 Ti ions replaced with Zr in 2x2x2 supercell to cover the entire compositional range. These simulations produced the equilibrium lattice constant as a function of Zr concentration, $a(x)$. The lattice constant was found to increase linearly with Zr concentration in agreement with another DFT study [12]. Next cubic lattice constant of $BaTiO_3$ was computed as a function of hydrostatic pressure, $a(P)$, in the range of 0 to -20 GPa. The data for $a(x)$ and $a(P)$ were used to compute the dependence of the negative pressure on Zr concentration.

The extended Hamiltonian was used in the framework of Molecular Dynamics (MD) to study finite-temperature properties of $Ba(Ti_{1-x},Zr_x)O_3$. Since many of the characteristic features of these solid solutions are believed to originate from dynamical and thermal fluctuations we believe that MD is the appropriate tool for investigation of their properties. Supercell sizes of 12x12x12, 20x20x20, and 30x30x30 were considered in order to address the effect of the supercell size. To trace the temperature evolution of the $Ba(Ti_{1-x},Zr_x)O_3$ properties the supercells were annealed from 450 K down to 10 K in steps of 10 K. Although we expect our approach to be accurate for low Zr concentrations we, nevertheless, carried out simulations in the entire compositional range. Several sets of simulations were

run with different number of the MD steps: 40,000 MD steps (Set 1), 100,000 MD steps (Set 2) and 600,000 MD steps (Set 3) to investigate the dynamical aspect of the properties. While for pure $BaTiO_3$ we did not find significant differences in the data between 20x20x20 and 30x30x30 supercell sizes and between different simulation Sets, it was not the case for $Ba(Ti_{1-x},Zr_x)O_3$ where we found dependence of the results on both supercell size and number of MD steps. In addition, the properties were also dependent on the particular random distribution of the Zr sites inside $BaTiO_3$ matrix. This is an indication of the complexity of the energy landscape for these solid solutions.

RESULTS AND DISCUSSION

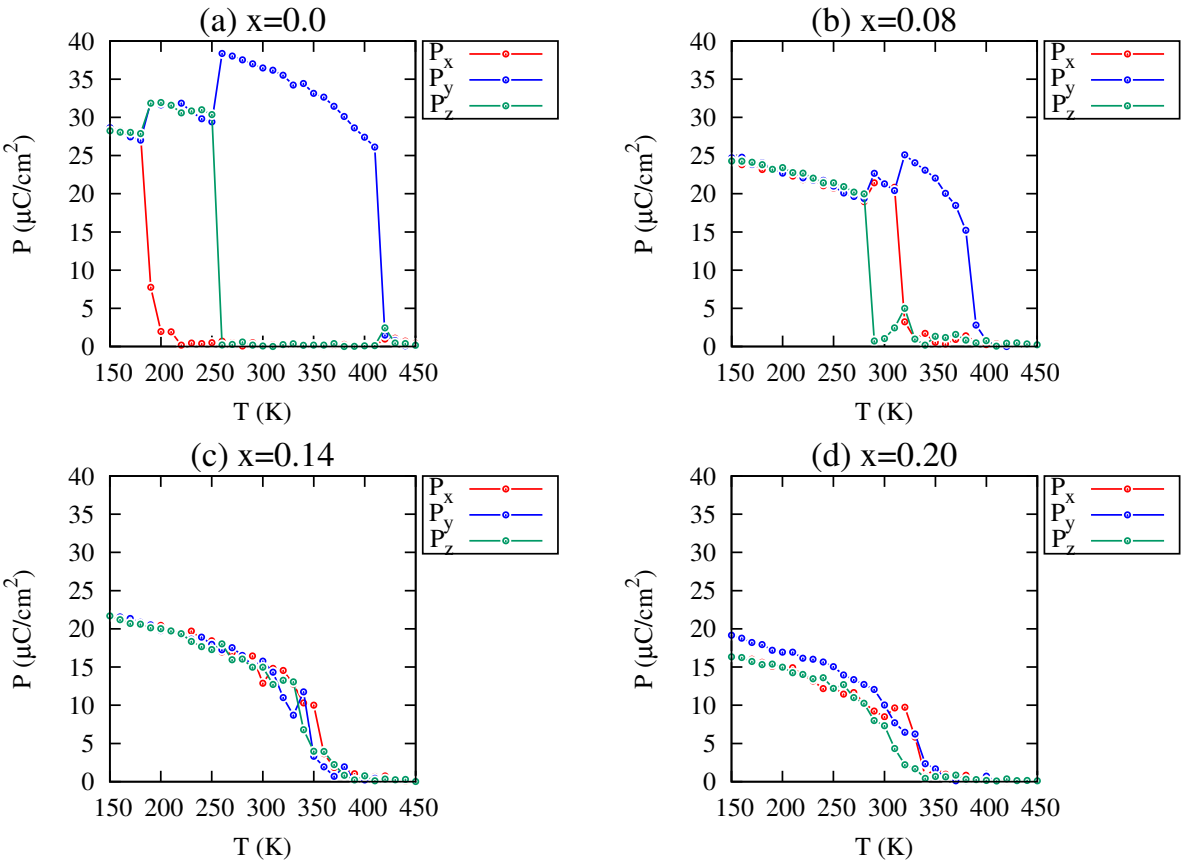

FIG. 3. Temperature evolution of polarization components for a few representative Zr concentrations.

Figure 3 shows a few representative dependencies of polarization on temperature, $P(T)$, from our annealing simulations (Zr concentrations 0.00, 0.08, 0.14 and 0.20, Set 2). As Zr

concentration increases the Curie temperature decreases and the three ferroelectric transitions come closer together and merge in agreement with experimental findings. The polarization decreases considerably in magnitude as Zr concentration increases. These data were used to obtain the dependence of the transition temperatures on Zr concentration which is given in Fig.4. Experimental data from the literature [20–22] are presented in the same figure. We find good agreement between the experimental and computational data. On the basis of the agreement we conclude that the mechanical and electrostatic effects of Zr substitution of Ti identified from DFT calculations are primarily responsible for the phase evolution in these solid solutions. Insets to Fig.4 show our computational data and

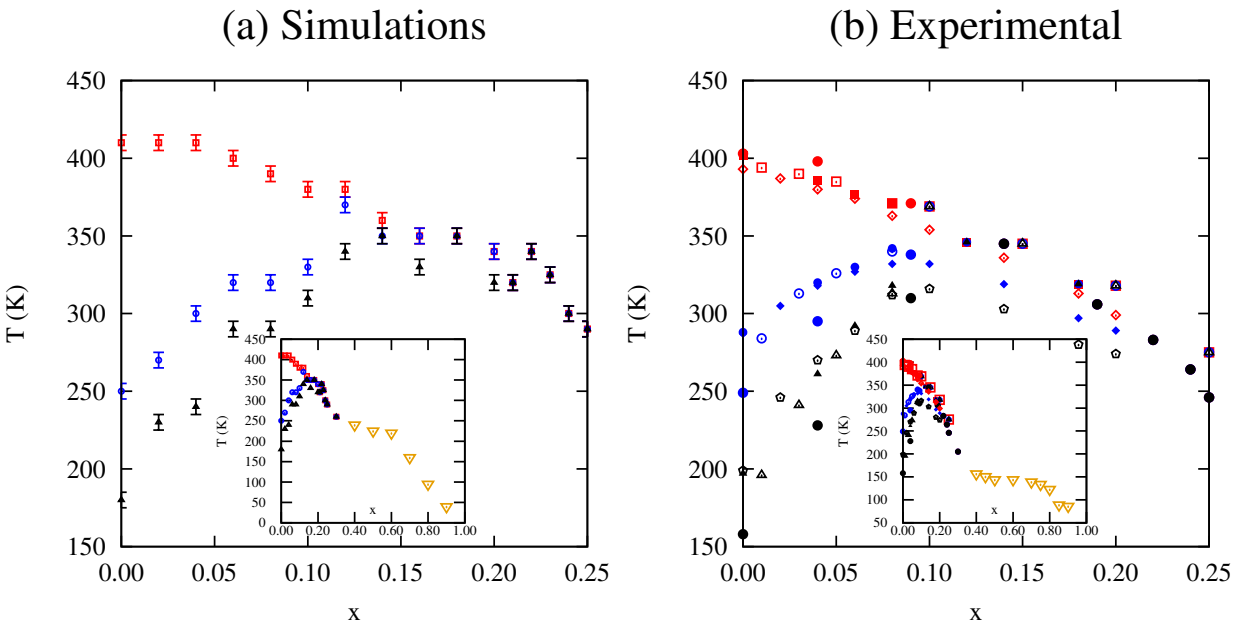

FIG. 4. Dependence of transition temperatures on Zr concentration obtained from computations (a), and experimental data from the literature [20–22](b). The insets give the data in the entire concentration range. Yellow triangles on the inset give T_m.

experimental data from the literature in the entire compositional range. For x >0.30 we find macroscopically nonpolar phase with T_m decreasing with x in striking agreement with experimental data.

To understand the microscopic origin for the observed features we investigate the dipole patterns at 150 K obtained from the Set 2. Some representatives are given in Fig.5. For Zr concentrations below the one associated with pinched transition we find a polar matrix with some defect-like inclusions. In the concentration range 0.18 to 0.35 of Zr we observe formations of nanoregions (Fig.5(b)-(d)) associated with different polarization orientation. Interestingly, however, some of these PNRs are not clusters but rather have a nanopillar geometry with the axis aligned along <001> direction and extending through the entire supercell. This is in agreement with the experimental reports of one-dimensional PNRs with anisotropic chain dipoles along <001> direction [23, 24]. In some cases we find interpenetrating pattern of these nanopillars. Such clusters develop gradually as the temperature decreases below the Curie point. In simulations, the presence of such PNRs may lead to the apparent monoclinic phase due to the finite size of the supercell as it happens in Fig3(d). For Zr concentrations of 0.50 and above the dipoles are completely disordered (see Fig.5(e)).

Interestingly, we found that the precise details of the phase evolution and the phase diagram given in Figs.3 and 4 depend on the number of MD steps which suggests that in the vicinity of phase transition the phases and PNRs evolve with time on the time scale of tenths nanosecond.

One of the open questions in ferroelectric relaxors is the nature of the difuse phase transition. In $Ba(Ti_{1-x},Zr_x)O_3$ it occurs for $0.15 \leq x \leq 0.20$. It was suggested [25] that the unusual behavior of the dielectric response in this region could be attributed to the overlapping of the three maxima in the dielectric response associated with the three ferroelectric phases (tetragonal, orthorhombic and rhombohedral). Most puzzling, however, is the fact that these unusual features continue to persist even for Zr concentrations above the one associated with pinched phase transition [25]. To investigate into that we study the response of the $Ba(Ti_{1-x},Zr_x)O_3$ with $x = 0.18$ to the applied *ac* electric field with frequency of 1 GHz. We have simulated three different directions of the electric field: [100], [110], and [111] in the temperature range of 280 to 380 K, which brackets the Curie point of 350 K. Simulation supercell 30x30x30 was used. The data for 280 and 320 K is given in Fig.6. Surprisingly, we find that in this solid solution it is possible to stabilize either one of the three ferroelectric phases of the parent $BaTiO_3$, namely tetragonal, orthorhombic or rhombohedral phase. This is manifestation of the fact that the free energies of these phases are rather

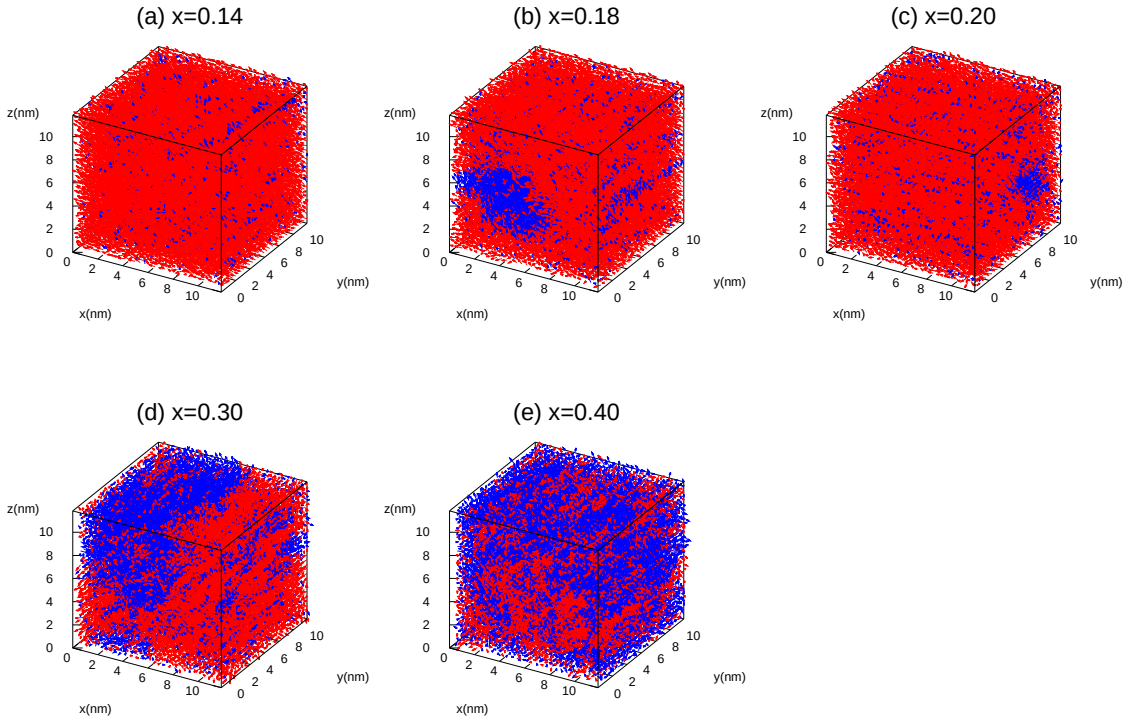

FIG. 5. Dipole patterns in the simulation supercells at 150 K. Different colors are used to visualize regions with polarization component of different directions.

close to each other. Furthermore the possibility to switch between the different phases by the application of electric field suggest high and rather unusual susceptibility which could be responsible for the enhanced dielectric response. Such property is extremely rare and highly desirable. Experimentally, it is expected to lead to the coexistence of all three ferroelectric phases [25]. Interestingly, we find that such phase competition occurs in the entire temperature range investigated which could explain the enhancement of the dielectric response in a wide temperature range and associated diffuse nature of the phase transition. Therefore, our data support the earlier hypothesis that the dielectric response in the region of diffuse phase transition could be attributed to the overlapping of the three maxima in the dielectric response associated with the three ferroelectric phases [25].

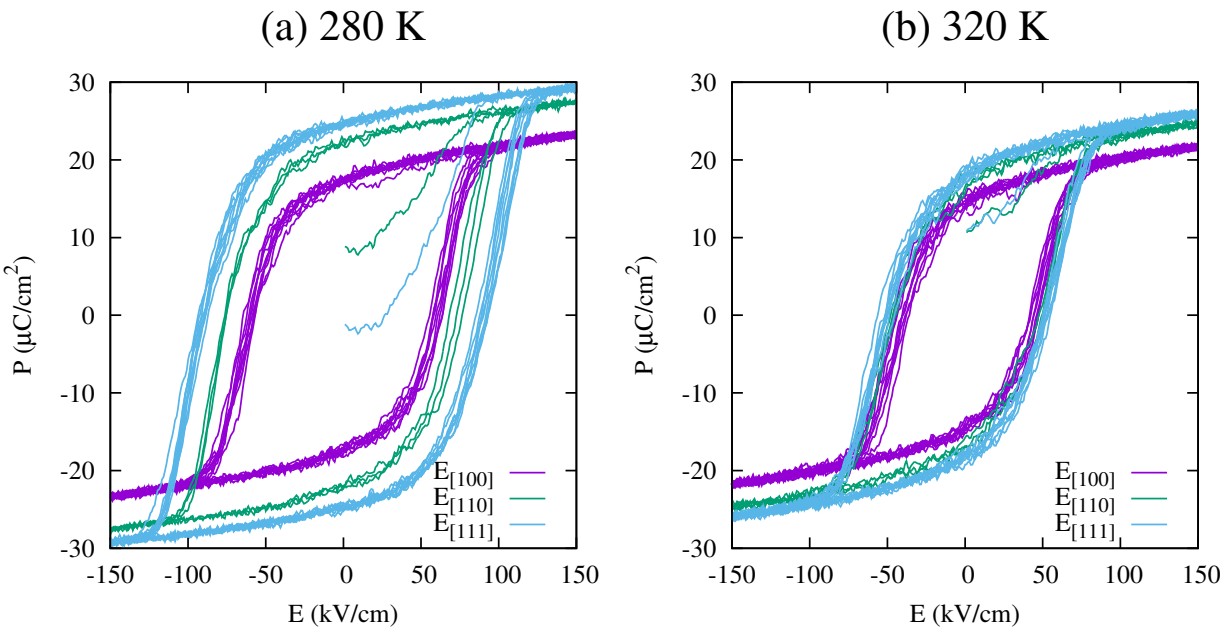

FIG. 6. The dependence of the polarization on the applied electric field for 280 K (a) and 320 K (b). The polarization component along the field direction is reported. Legend give the direction of the applied electric field.

CONCLUSIONS

We have investigated phase evolution in $Ba(Ti_{1-x},Zr_x)O_3$ solid solution using a combined first-principles DFT and first-principles-based effective Hamiltonian approach. From DFT computations we found that Zr substitution of Ti leads to (i) lattice expansion of the $BaTiO_3$ matrix, which could be described as negative chemical pressure, and (ii) weakening of ferroelectric cooperation due to the inability of Zr ion to undergo collective ferroelectric distortion. These findings were used to extend the effective Hamiltonian for $BaTiO_3$ to the case of $Ba(Ti_{1-x},Zr_x)O_3$. Surprisingly, we found that the extended effective Hamiltonian predictions are in excellent agreement with experimental phase diagram in the entire range of Zr concentration, which demonstrates that the two aforementioned effects of Ti substitution with Zr are primarily responsible for the phase evolution in this family of

solid solutions. In particular, our methodology accurately predicts pinched phase transition whose existence we attribute to the same competition between the stabilizing effect of negative chemical pressure and destabilizing effect of "ferroelectricaly nonactive" Zr. In the region of concentrations associated with the diffuse phase transition we found PNRs with different polarization direction. These nanoregions often have nanopillar geometry with the axis along <001> direction. Furthermore, in this region we find that either one of the three ferroelectric phase of the parent $BaTiO_3$ can occur, which could explain the enhanced susceptibility to the electric field (large and broad dielectric response). For concentrations x >0.30 we find macroscopically nonpolar phase with T_m decreasing with x. For concentrations x >0.50 the dipoles are completely disordered in the absence of the electric field. We believe that our study advances current understanding of the ferroelectric relaxors without nominal charge disorder and the proposed computational methodology will allow for many future investigations into such solid solutions.

ACKNOWLEDGMENTS

The present work is supported by the U.S. Department of Energy, Office of Basic Energy Sciences, Division of Materials Sciences and Engineering under grant DE-SC0005245. Computer time was provided by USF Research Computing, sponsored in part by NSF MRI CHE-1531590.

[1] K. Uchino, *Ferroelectric Devices* (New York: Dekker, 2000).

[2] S. R. Anton and H. A. Sodano, Smart Mater. Struct. **16**, R1 (2007).

[3] V. V. Shvartsman and D. C. Lupascu, J. Am. Ceram. Soc. **95**, 1 (2012).

[4] V. V. Lemanov, E. P. Smirnova, P. P. Syrnikov, and E. A. Tarakanov, Phys. Rev. B **54**, 3151 (1996).

[5] C. Ménoret, J. M. Kiat, B. Dkhil, M. Dunlop, H. Dammak, and O. Hernandez, Phys. Rev. B **65**, 224104 (2002).

[6] W. Xiaoyong, F. Yujun, and Y. Xi, Appl. Phys. Lett. **83**, 2031 (2003).

[7] V. V. Shvartsman, J. Zhai, and W. Kleemann, Ferroelectrics **379**, 77 (2009).

[8] A. R. Akbarzadeh, S. Prosandeev, E. J. Walter, A. Al-Barakaty, and L. Bellaiche, Phys. Rev. Lett. **108**, 257601 (2012).

[9] S. Prosandeev, D. Wang, A. R. Akbarzadeh, B. Dkhil, and L. Bellaiche, Phys. Rev. Lett. **110**, 207601 (2013).

[10] H. Takenaka, I. Grinberg, and A. M. Rappe, Phys. Rev. Lett. **110**, 147602 (2013).

[11] D. Wang, J. Hlinka, A. A. Bokov, Z. G. Ye, P. Ondrejkovic, J. Petzelt, and L. Bellaiche, Nat. Commun. **5**, 5100 (2014).

[12] D. Amoroso, A. Cano, and P. Ghosez, Phys. Rev. B **97**, 174108 (2018).

[13] G. Kresse and J. Furthmüller, Phys. Rev. B **54**, 11169 (1996).

[14] P. E. Blöchl, Phys. Rev. B **50**, 17953 (1994).

[15] R. D. King-Smith and D. Vanderbilt, Phys. Rev. B **47**, 1651 (1993).

[16] H. H. Wieder, Phys. Rev. **99**, 1161 (1955).

[17] R. Herchig, C.-M. Chang, B. K. Mani, and I. Ponomareva, Sci. Rep. **5**, 17294 (2015).

[18] W. Zhong, D. Vanderbilt, and K. M. Rabe, Phys. Rev. B **52**, 6301 (1995).

[19] For Zr we used ξ_{Ti}.

[20] J. Ravez, C. Broustera, and A. Simon, J. Mater. Chem. **9**, 1609 (1999).

[21] A. Peliz-Barranco, ed., "Ferroelectric materials: Synthesis and characterization," (Intech, 2015) Chap. Role of Ca off-Centering in Tuning Ferroelectric Phase Transitions in Ba(Zr,Ti)O_3 System.

[22] L. Dong, D. S. Stone, and R. S. Lakes, J. of Appl. Phys. **111**, 084107 (2012).

[23] Y. Liu, R. L. Withers, X. Wei, and J. D. F. Gerald, J. Solid State Chem. **180**, 858 (2007).

[24] Y. Liu, R. L. Withers, B. Nguyen, and K. Elliott, Appl.Phys. Lett. **91**, 152907 (2007).

[25] D. Hennings, A. Schnell, and G. Simon, J. Am. Ceram. Soc. **65**, 539.